Feasibility Study of a Light Weight Solar Powered Train: Case of Addis Ababa Light Rail Transit (AALRT)

Nibaruta Regis*, Mugisho Mugaruka Josue

1 Traction and Train Control Program, African Railway Center of Excellence Addis Ababa University, Ethiopia,
2 Traction and Train Control Program, African Railway Center of Excellence Addis Ababa University, Ethiopia,

IJASR 2021
VOLUME 4
ISSUE 2 MARCH – APRIL **ISSN: 2581-7876**

Abstract: This paper presents a study of the feasibility of a solar powered light weight urban train that can be adapted to the existing electrical Addis Ababa Light Rail Transit (AALRT) in Ethiopia. The structure proposed in this paper is to install the solar panels on the train's roof with possible onboard batteries. A demand-supply analysis has been carried out in this study to compute the energy exchange, taking into account the available area of a railcar roof for the photovoltaic (PV) energy production and the regenerated energy during train braking. Results of this study show that an optimally sized PV system can be integrated as an alternative supply. The computations have shown that out of the 1,816.57kWh consumed daily by a single train vehicle, 814.8 kWh which is 44.85% can be covered by the PV energy together with regenerative energy. The utility grid can supply the 55.15% shortage equivalent to 1,001.77 kWh. Results also demonstrate that the overall energy production always falls below the required energy and energy storage is not required for our particular case study. The feasibility and functional effectiveness of this analysis are illustrated using the data collected along the West-East line of the AALRT.

Keywords: Addis Ababa Light Rail Transit, Renewable Energy, Energy demand, Solar train, Energy supply

1. Introduction

The increased attention in the utilization of energy storage technologies to enhance the functioning of tramways has triggered evolving verification methods and excellent energy storage units in order to glean profits and lower the cost of installation. [1]. recently, the quick expansion of photovoltaic energy as renewables has also fuelled the substantial interest in coupling renewable energy and storage units. Solar photovoltaic (PV) deployment on existing train's rooftops has proven to be one of the most viable large-scale resources of sustainable energy for urban trains [2].

Preserving quality and secure electrical utility services while tempting to quickly decarbonize electric power systems is a major issue/challenge for countries around the world. While renewable energy offers a clean and cheaper energy supply, it is of practical importance to investigate the applicability of solar PV systems with storages Which may produce sufficient electrical energy for the AC and DC electrical locomotives and other equipments [3]. It has been suggested in [4] that batteries, flywheels and supercapacitors are the three main storage technologies used in railway. In the railway industry, Traction energy consumption keeps rising and it is believed that railway electric systems could be powered by track-connected solar which is not only cheaper but also low carbon that utility grid energy [5]. The transport industry is among the chief contributors of greenhouse emissions. It contributes approximately 13.4% of the total contribution of greenhouse emissions [6].

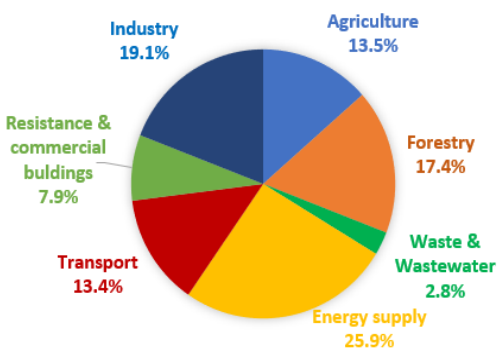

Figure 1. Percentage contribution of various sectors towards greenhouse emissions

Electric railway lines present significant novel market businesses and opportunities that could unfold fresh commercial development of solar energy technology in Africa and beyond [5]. In many developing countries, the reliable access to electricity is still a big challenge and about 55.7% of Ethiopians still have no access to the national electric grid or any other significant electricity source [7], [8]. They depend on dry-cell batteries, or off-grid electrical energy supply which does not cater enough ancillary services or basic energy needs. The total average energy consumed daily by one train vehicle is about 1.8MWh totalling a daily consumption of 36MWh for the 20 train vehicles on the E-W line of the AALRT when all are operating. This energy could be used to supply some of the Ethiopians who have no access to electricity at all.

The main purpose of this study is not to entirely eliminate the conventional energy supply but to alternatively propose an integration of photovoltaic energy supply in order to limit/decrease the overloading of traction subsystems, therefore lowering the power consumption. Climate change continue to upset the world and alternative ways of producing energy is being extensively researched on. There is a substantial need to reduce carbon emission in public transport and railway systems should not be left behind in this transformation. Authors in [9] studied the feasibility of a hydrogen-powered train in an attempt to reduce carbon emission. Public transport must be eco-friendlier and more solar plane on roof of train could produce much of the required power [10].

1. Methodology

This section presents the methodological steps and procedures followed to achieve the objectives of this study. Regenerative braking energy and hourly solar energy gain (PV) are modelled and computed as contributory sources to train energy requirement. Different forces acting on the train motion are also computed to perform the train demand-supply analysis. Energy exchange analysis is finally performed to find out the necessity of installing supercapacitor batteries.

2.1. Regenerative Braking Energy Modelling

Today's advanced electric train systems are fitted out with regenerative braking systems in which some energy is generated from the train's kinetics during the braking. Note that the train's braking force is composed of friction braking force and motor braking force which is the force the motor uses to generate electricity. Thus, the product of the motor braking force, velocity and regenerative efficiency yield the electric power produced by the regenerative braking. It can be expressed as in [11], [12] as follow:

$$P_{reg} = F_b \times V \times \eta_{reg}, \qquad (1)$$

where P_{reg} is the electric power regenerated from braking (kW), F_b is the regenerative braking force (kN), V is the speed of the train (m/s), η_{reg} is the efficiency of the regeneration system.

The power consumed during braking and regenerated power can be estimated based on the traction braking force which acts to decelerate and stop the train and has been expressed in [12] as:

$$\begin{aligned} M_{tot}\beta &= -\left(F_b + F_g + F_r\right) \\ -F_b &= M_{tot}\beta + F_g + F_r, \end{aligned} \qquad (2)$$

where M_{tot} is the total mass; F_b is the braking force (N); F_g is the force required to overcome the gravity; F_r is the force required to overcome train resistance and β is decerelation (m/s^2)

The consumed power to halt the motion is equal to the product of braking force FB, and the change in velocity gives the power to be provided for braking:

$$P_{cons} = F_b + \Delta V, \qquad (3)$$

Where P_{cons} is the power consumed during braking and ΔV is the change of speed during braking to stop.

It is possible to calculate the regenerated power for a break at stations as:

$$P_{reg} = P_{cons} \times \eta_{reg},$$
$$\eta_{reg} = \frac{1}{(e^{\frac{\alpha}{|a|}})}, \quad (4)$$

where α is the Optimum model parameter (commonly used as 0.65 for Asynchronous motor-driven machines), a is the maximum deceleration of the vehicle.

Regenerated energy is calculated by integrating the power over the braking time [11]:

$$E_{reg} = \int P_{cons} dt. \quad (5)$$

Form this regenerative braking energy model; it is clear that its magnitude depends on a combination of many factors including efficiency of regeneration, braking time, deceleration, train mass, maximum operational speed, and all resistive forces. In the next step, we present the solar PV mode equivalent circuit and its parameters.

2.2. Equivalent Circuit of Solar PV module

The equivalent circuit diagram of solar PV module is shown in Figure 2. The current I at the output terminals is represented by the subtraction of the diode current I_d and the shunt current I_{sh} from the generated light current I_l. Rs which is the series resistance symbolize the internal resistance of the current flow. It is a function of the pn junction depth, impurities, and contact resistance. The shunt resistance R_{sh} is pertaining to the leakage resistance to ground[3]

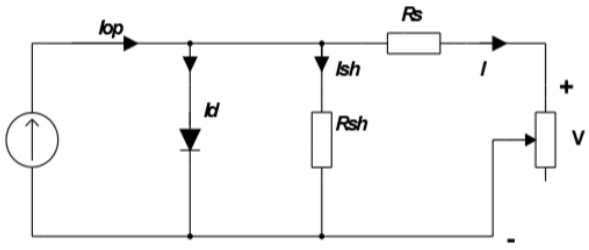

Figure 2. Equivalent circuit diagram of solar PV module

$$R_{pv} = -M\frac{I_{sc}}{I_{MPP}} + \frac{V_{MPP}}{I_{MPP}}\left(1 - \frac{I_{sc}}{I_{MPP}}\right),$$
$$V_T = -(M + R_{pv})I_{sc}, \quad (6)$$
$$I_0 = I_{sc}\, e^{\frac{V_{oc}}{V_T}},$$
$$I_{ph} = I_{sc}.$$

where R_{pv} is the PV resistor; I_{ph} is the photon current; I_{sc} is the short circuit current; I_{MPP} is the maximum power point current; V_{MPP} is the maximum power point voltage; V_{oc} is the open circuit voltage

The gradient M is required for the calculation. It is a function of the following parameters:

$$M = f(V_{oc}, \quad I_{sc}, \quad V_{MPP}, \quad I_{MPP})$$

The following approximation of the characteristic curve can be derived with an accuracy of 1%.

$$M = \frac{V_{oc}}{I_{sc}}\left(K_1 \frac{I_{MPP}\, V_{MPP}}{I_{sc}\, V_{oc}} + K_2 \frac{V_{MPP}}{V_{oc}} + K_3 \frac{I_{MPP}}{I_{sc}} + K_4\right) \quad (7)$$

With the equation constants:

$$K_1 = -5.411$$

$$K_2 = 6.450$$

$$K_3 = 3.417$$

$$K_4 = -4.422$$

2.3 Insolation computation of tilted surface

To calculate the amount of energy generated by photovoltaic panels, the hourly solar energy gain is predicted using the isotropic model presented in [14]. In this model, both azimuth and inclination angle are considered. Hourly radiation on an inclined surface can be obtained using equation (8) [15]:

Total daily radiation on an horizontal surface in outer atmosphere □□□□ is expressed as following:

$$H_{ext} = \frac{24}{\Pi} \Phi_{ext}\, cos\, cos\, \delta \; cos\, cos\, \lambda \; [sin\, sin\, \omega_{ss} - \omega_{ss}\, cos\, cos\, \omega_{ss}] \quad (8)$$

where Φ_{ext} is solar constant (1370w/m2); δ is solar declination angle; λ is the latitude and ω_{ss} is the sunset hour on the horizontal

Solar declination at any day of the year is expressed as:

$$\delta = 23.45\, sin\left(360 \cdot \frac{284 + n}{365}\right) \quad (9)$$

where n is the number of days in each month

Hour angle at sunrise/sunset:

$$\omega_{sunrise/sunset} = \omega_{ss} = arcos\,[-\, tan\, tan\, \delta \;\; tan\, tan\, \lambda\,]$$

Hour angle at sunrise/sunset on a tilted surface:

$$\omega'_{ss} = a\, cos\, cos\,[-\, tan\, tan\, \delta \; tan\, tan\, (\lambda - \beta)\,] \quad (10)$$

Clearness index:

$$K_T = \frac{H}{H_{ext}} \quad (11)$$

Total daily solar energy flux (kwh/m2) onto a surface tilted:

$$H_\beta = R.H$$

$$R = \left[1 - \left(\frac{H_d}{H}\right)\right].R_b + \left(\frac{H_d}{H}\right).\left(\frac{1 + cos\beta}{2}\right) + \rho.\left(\frac{1 - cos\beta}{2}\right) \quad (12)$$

where H is horizontal irradiation (kW/m2/day); H_d is the daily diffuse radiation; β is the surface inclination angle; ρ is correction coefficient (0.25)

$$R_b = \frac{H_{ext}(\beta)}{H_{ext}} = \frac{cos\delta\ cos\ cos\ (\lambda-\beta)[sin\ \omega'_{ss} - \omega'_{ss}cos}{cos\delta cos\lambda[sin\omega_{ss} - \omega_{ss}cos\omega_{ss}]} \quad (13).$$

where ω'_{ss} is the sunset hour on a tilted array

Liu & Jordan equations [14]

$$w_s \leq 81.4° \quad 0.3 \leq K_t \leq 0.8$$
$$\frac{H_d}{H} = 1.391 - 3.560 \cdot K_t + 4.189 \cdot K_t^2 - 2.137 \cdot K_t^3$$
$$w_s \geq 81.4° \quad 0.3 \leq K_t \leq 0.8 \quad (14)$$
$$\frac{H_d}{H} = 1.311 - 3.022 \cdot K_t + 3.427 \cdot K_t^2 - 1.821 \cdot K_t^3$$

2.4 Train demand Supply analysis

In order to compute the energy requirements for a train operating on a defined track, the standard equations of motion are applied. To apply these equations, the force acting against the train movement has to be taken into account. These forces include rolling resistance, resistance due to aerodynamic drag, resistance due to acceleration and resistance due to gradient. For simplicity, in this model, we will consider three opposing forces namely: acceleration force, train motion resistance and resistance due to the gradient. The tractive effort required for train propulsion is expressed in [16] as:

$$F_t = F_a + F_g + F_r \quad (15)$$

where F_a is the force required for giving linear acceleration to the train.

2.4.1 Force required to overcome resistance due to acceleration (Fa).

As stated by the Newton second law of motion, the force required to accelerate the train in motion is given by:

$$Force\ =\ Mass\ \times\ acceleration \quad (16)$$

The fact that the train has rotating parts such as motor armature, wheels, axels, and gear system, its mass including the mass of rotating parts is known as effective mass or accelerating mass (Me) and is much higher (about 8–15%) than its stationary mass (M). Hence, these parts need to be given angular acceleration at the same time as the whole train is accelerated in a linear direction. Thus, the equation above becomes:

$$F_a = M_e \times \alpha \quad (17)$$

When the train effective mass M_e is expressed in kg and acceleration α expressed in m/s2 the above equation becomes:

$$F_a = 1000 M_e \left(\frac{1000}{3600}\right) \alpha \left(\frac{kg-m}{s^2}\right) \quad (18)$$

Therefore, the force required for a linear and angular acceleration is [16]:

$$F_a = 277.8 M_e \times \alpha \quad (N) \quad (19)$$

2.4.2 Force required overcoming the train resistance (Fr).

When the train is running at uniform speed on a level track, it has to surmount the opposing forces due to the surface friction, i.e., the friction at various parts of the rolling stock, the fraction at the track, and also due to the wind resistance. Parameters that affect or determine the size of the frictional resistance include shape, size, track conditions, train speed, etc. Considering r as specific resistance, the force required to overcome this resistance is:

$$F_r = Mr, \quad r = \frac{R}{M} \quad F_r = R. \quad (20)$$

The total resistance against the train movement is given by Davis equation:

$$R = 1.3W + 29N + b \times W \times V + c \times A \times V^2 \quad (21)$$

Where R is the total resistance in lbs. (1lbs = 4.45N); W is the train weight in tones; N is the number of train axles; V is the train speed in miles/hour; b is the experimental friction coefficient (for passenger car b = 0.03); c is drag coefficient (for passenger car); A is the cross section of train frontal area (square feet); At maximum speed (70km/h equivalent to 112 mph)

2.4.3 The force required to overcome the gradient resistance (Fg).

When the train is moving on up gradient, Figure 3, the gravity component of the dead mass opposes the motion of the train in an upward direction. In order to prevent this opposition, the force should be acting in an upward direction [16].

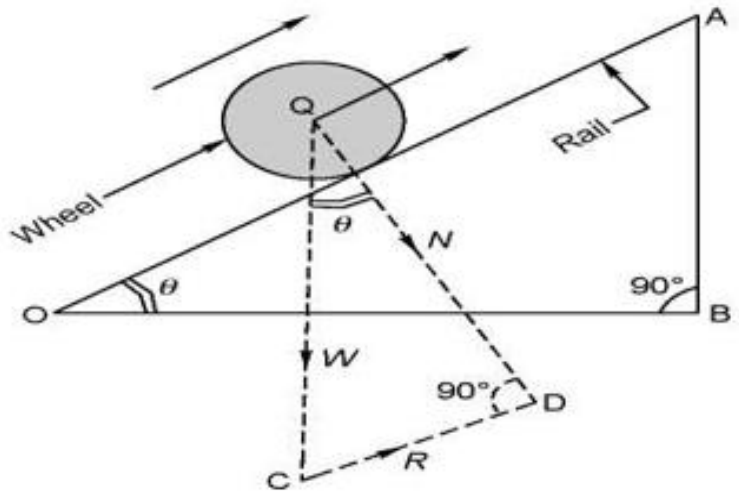

Figure 3. Resistance due to gradient

Considering an uphill motion of the train,

the force required to overcome the resistance due to gravity is:

$$F_g = M_g \, sin \, sin \, \theta \tag{22}$$

In railway practice, the gradient is expressed as the rise (in meters) a track distance of 100m and

is called "percentage gradient".

$$\%G = \frac{\frac{BC}{AC}}{100} = 100 \times \frac{BC}{AC} = 100 \, sin \, sin \, \theta \tag{23}$$

Substituting the value of $sin \, sin \, \theta$, the equation becomes:

$$F_g = M_g \frac{C}{100} \tag{24}$$

When the mass is expressed in kg, the force to overcome gradient becomes:

$$F_g = 9.81 \times 10^{-2}(1000MG)$$

$$= 98.1MG \;\; (Newton)$$

2.4.4 Train Energy Consumption

The train energy consumption calculation requires detailed train running states outputted from train performance simulator (TPS) or speed profile generator, including train speed, running time, corresponding tractive effort and braking force. The model employs a numerical integration method to estimate the overall energy consumption of a single train operation. It can be found by dividing the energy output of the driving axles with the combined efficiency of transmission gear and motor [17].

$$E_{cons} = \frac{E_{output \; from \; driving \; axles}}{\eta_{motor} \cdot \eta_{gear}} \;\; (Wh) \tag{25}$$

By considering the efficiency of the traction inverter, we have:

$$E_{cons} = \frac{E_{output\ from\ driving\ axles}}{\eta_{motor} \cdot \eta_{gear} \cdot \eta_{inv}} \ (Wh) = \frac{0.01072 V_m^2 M_e + 27.25 MGD' + 0.2778 M_r D'}{\eta_{motor} \cdot \eta_{gear} \cdot \eta_{inv}} \quad (26)$$

Where V_m is expressed in km/h; M and Me in tones and r is expressed in N/tone. By applying the basic motion equations, outlined above, it is possible to determine the train power, energy, speed, etc.

Determining these parameters will enable quantifying the size and type of the energy flow (exchange) system to fit the purpose required.

Table 1 Train specifications at AALR

NO.	PARAMETER	VALUE
1	Train car weigh	44tone
2	Vehicle Car weight with full passenger 6persons/m2	59.24tone
3	(With 8 persons/m2)	(63.02tone)
4	Vehicle length (single vehicle)	29.4m
5	Car body width	2.65m
6	Maximum operation speed	70km/hr
7	Operation base speed	40km/hr
8	Acceleration under rated load (from 0-40km/hr)	1m/s2
9	Acceleration under rated load (from 0-70km/hr)	0.5m/s2

2.5. Number of PV panels calculation

The total area of the roof of an AALRT vehicle that operates on the E-W line is calculated in this section and the evaluations takes into account the train dimensions reported in Table 1. Taking into account the potential maximum distribution of the panels on the roof, according to Figure 4, it would be possible to place about 28 solar panels, in the arrangement described in table 2 above.

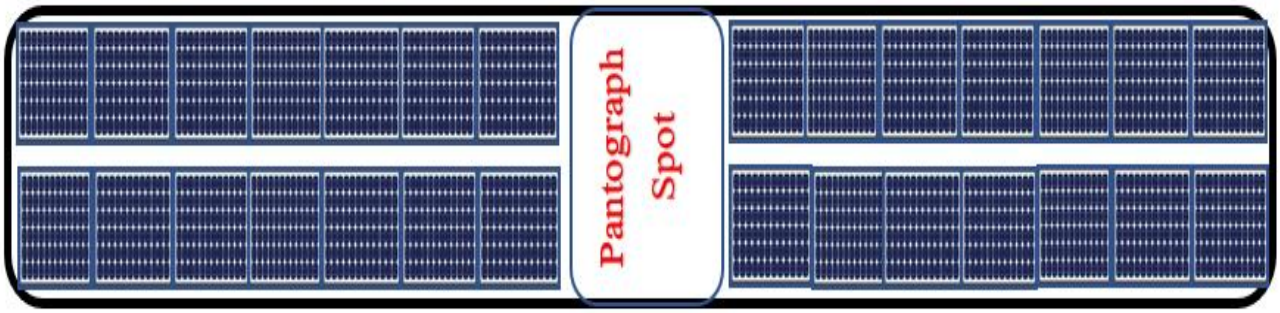

Figure 4. Distribution of the panels on the roof

Table 2 Number of PV panels calculation and arrangement

Total roof Area	$29.4m \times 2.65m = 77.91\ m^2$
For 72 cells,	
One Solar Panel Area	$1.965m \times 0.99m = 1.95\ m^2$
No. of Solar Panels	$\frac{77.91}{1.95} = 39.95$
14 panels longitudinally	$14 \times 1.965m = 27.51m < 29.4m$
2panels transversally	$0.99m \times 2 = 1.98m < 2.65m$

It is very necessary to compute the total weight of the PV panels because placing panels on the roof of the rolling train alter the total weight, thus increasing the energy consumption.

The Weight of one PV panel is 22 kg and total mass is obtained by multiplying the mass of one panel by the number of available PV panels Thus,

$$Total\ Weight = 22kg \times 28 = 616kg = 0.616\ tonne.$$

This mass must be taken into consideration while calculating the real energy consumption by train.

2.6. Photovoltaic energy production, according to the number of PV panels

The average horizontal radiation value in Addis Ababa and surrounding is around 6kWh/(m2xd), in other words: in the course of an average day (approximatlety13 hours from sunrise to sunset) the total energy radiated by the sun onto 1 square meter is 6 kWh. We would obtain the same amount of energy if radiation exposure was compressed, so to say 6 hours and the STC standard radiation of 1kW/m2 was radiated onto a surface of 1 square meter. With this in mind it is now possible to provide an interpretation of the measure of the module output Watt-peak (Wp).

Let us consider a 320 Wp module that lies flat on the roof of the moving train as a key of our study. The module would supply its peak output, also referred to as nominal output of 320 Watts for 6 hours. This would result in daily yield energy of 320 W x 6 hours= 1 920Wh/d

With 28 PV panels we have 1 920Wh/d x 28 =53.760 kWh/day

This energy is produced without taking into consideration the loss due to shadow effect.

3. Results and Discussion

A range of data and inputs variables has been utilized to come up with a reasonable analysis for the feasibility of the proposed system. The results presented in this part range from simple computation of energy requirements to complex calculations and energy exchange within the system.

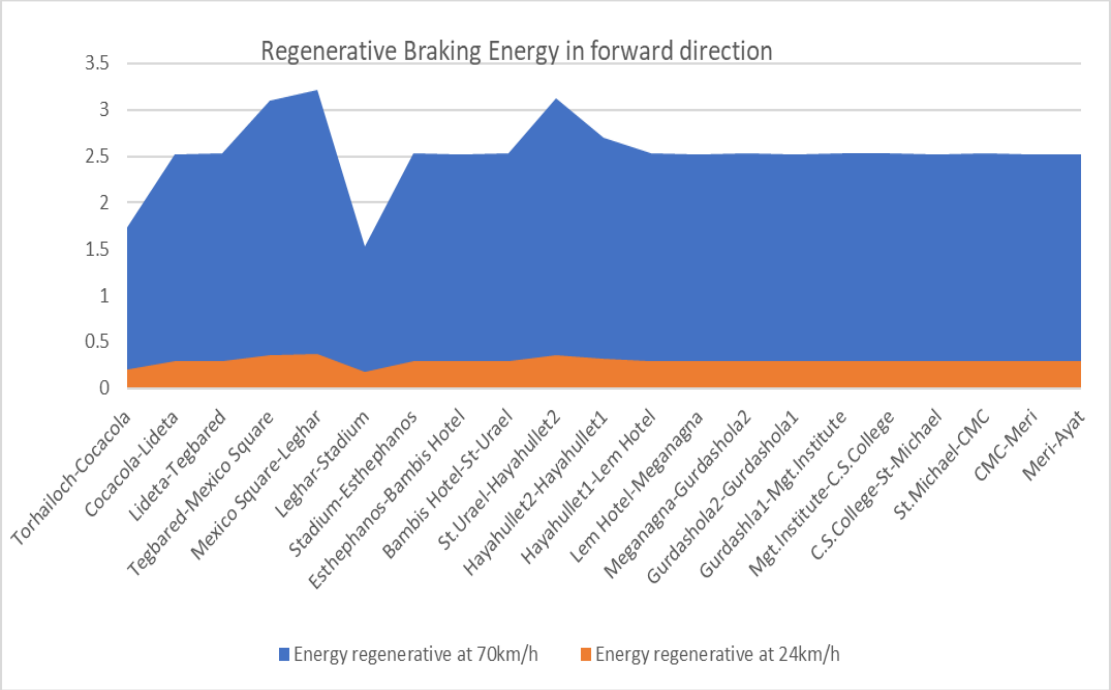

Figure 5. Regenerative braking energy in forward direction

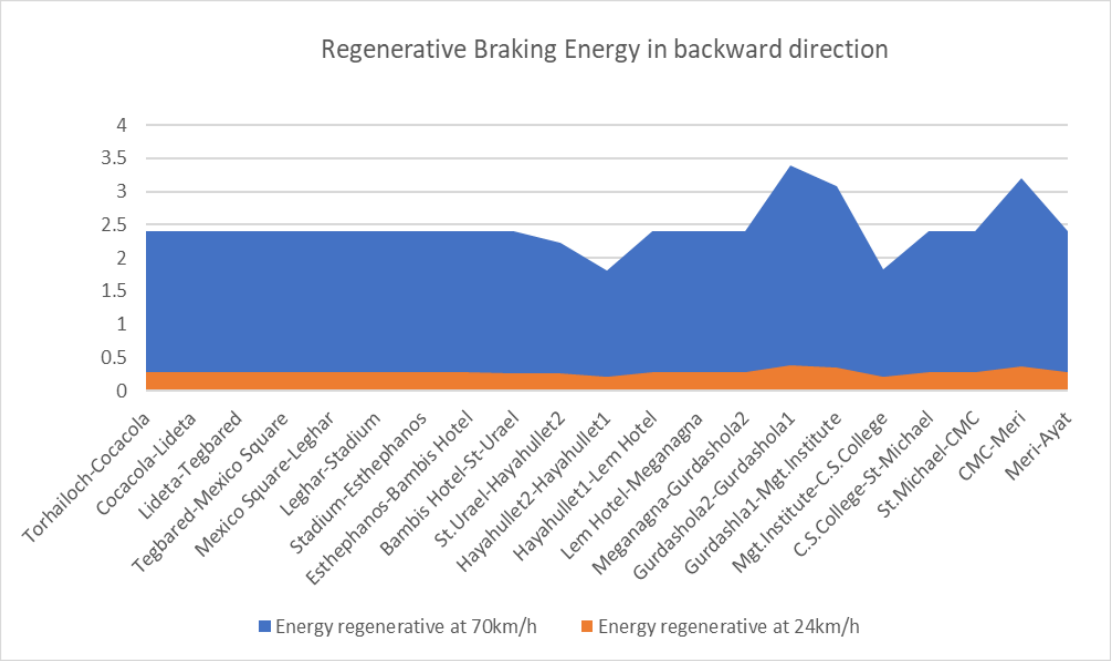

Figure 6. Regenerative braking energy in Return direction

Figures 5 and 6 present the variations of regenerative braking energy in forward and return direction respectively. From these figures we can realize that the train generates higher energy during braking period when running at the speed above the average. Relatively high energy consumption is also observed with this high speed whereas low energy consumption is observed for the speed below the average.

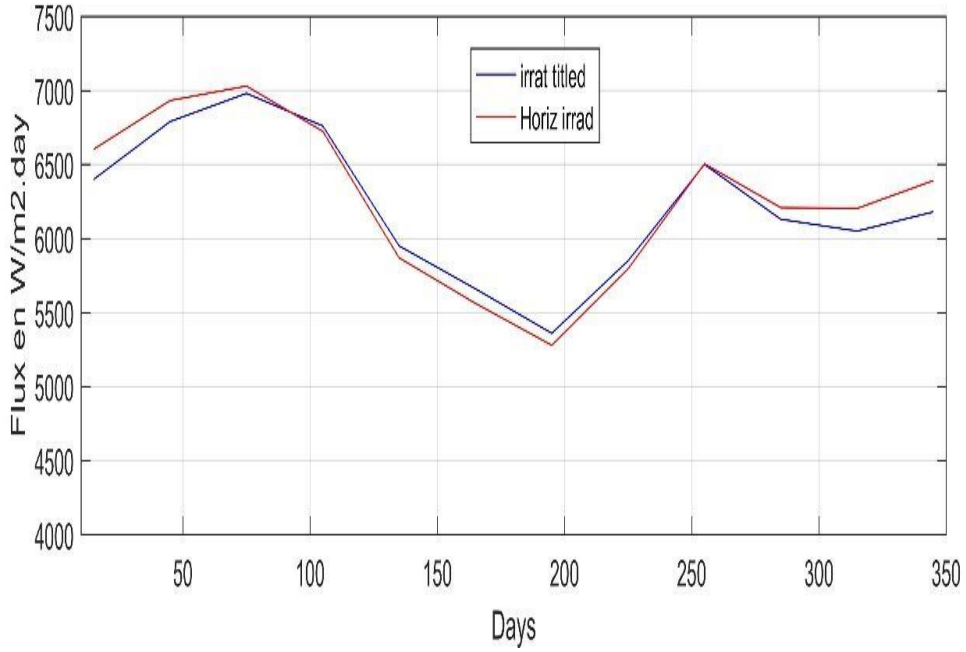

Figure 7. Comparison of irradiation between a horizontal and a tilted surface (30)

The figure 7 shows the variation of the annual irradition (insolation) when tilted with 30 for the Addis Ababa city located at 9.0110, 38.7610 Latitude/Longitude. From the same figure we see that the output energy is variable with the tilted angle but fluctuated around the horizontal plane.

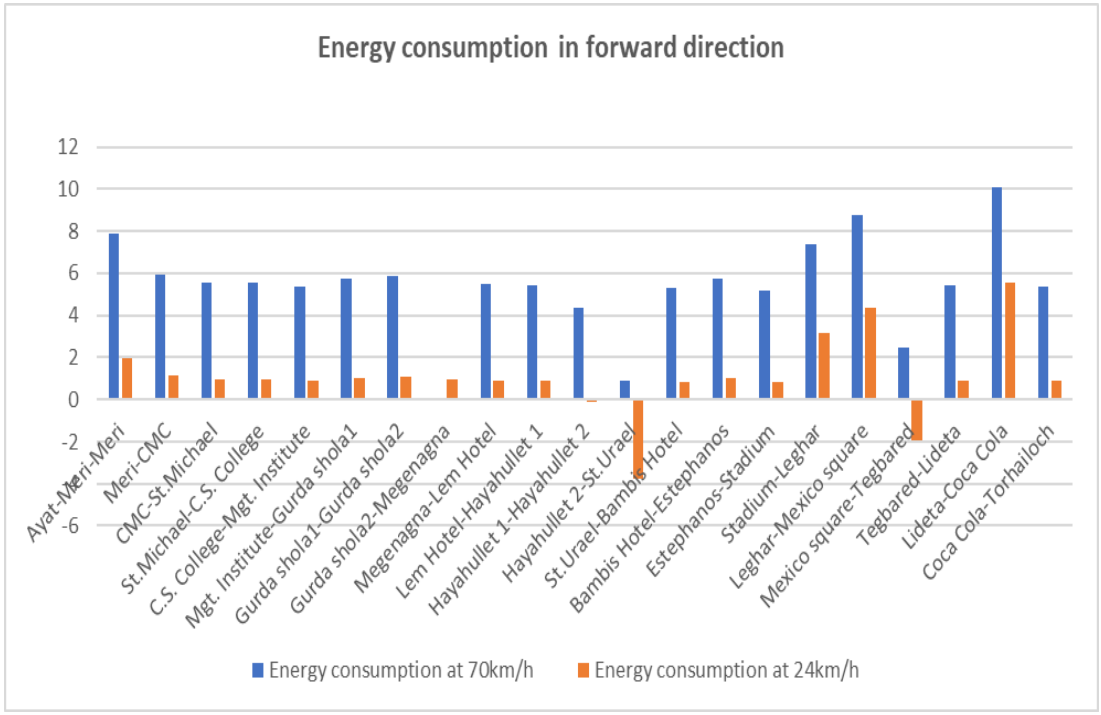

Figure 8. Energy consumption of the E-W line in the forward direction

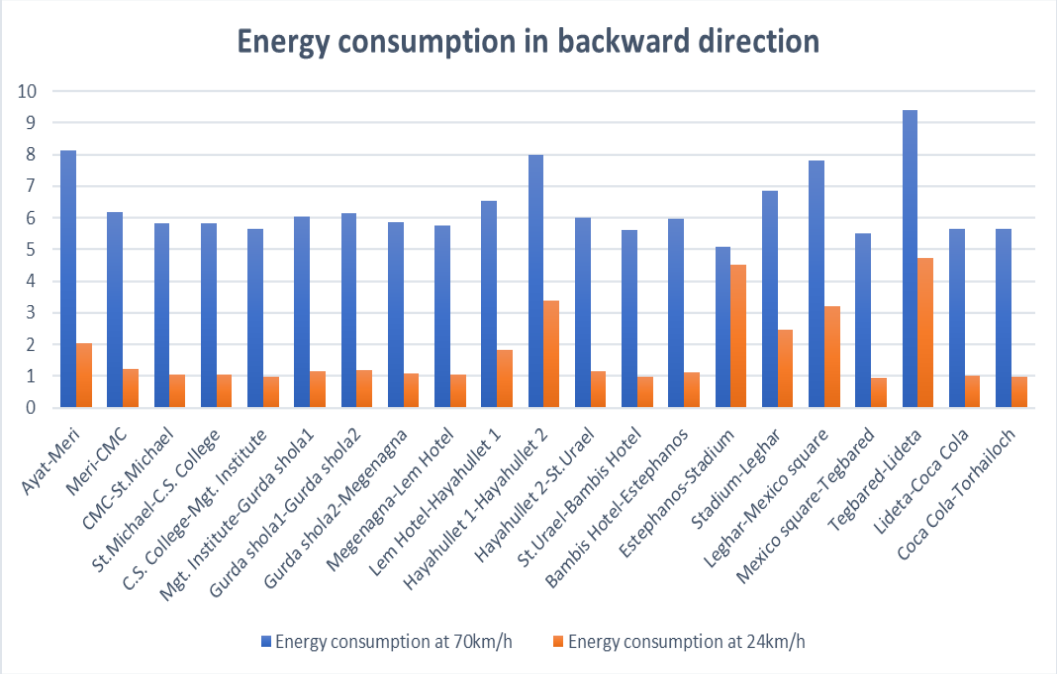

Figure 9. Energy consumption of the E-W line in Return direction

The train energy consumption depends on the magnitude of the gradient and the direction of travel. Results in Figure 8 and Figure 9 show the energy consumed when ascending a gradient is different from the consumed energy when descending that gradient, reason why the calculated energy consumption was computed for both direction of the East-West line of AA-LRT. The reason why there are negative values in the calculated energy consumption (figure 9), is that the regenerated energy which flows from traction motor to the catenary is greater than the energy drawn from the catenary to overcome the acceleration and resistance. The supplying source is designed considering the direction with the highest consumption (worst case scenario).

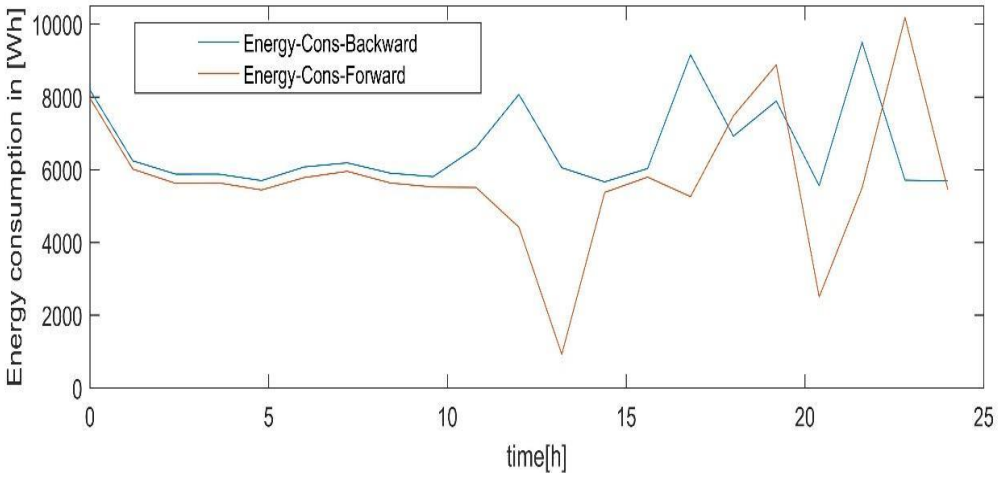

Figure 10. Energy consumption comparison after adding PV panels (Return & forward)

One round energy consumption by the train both forward (red) and Return (blue) is presented in Figure 10. Fluctuations observed in the energy consumption result from the fact that energy consumption depends on two key parameters considered in this project, namely the gradient and the distance for braking. We realize that there is a positive slope in Return while the forward direction is characterized by a negative slope. The difference is related to the topology of the train's trajectory in both directions. In the last part of both curves, the two slopes are proportionally increasing, and the peak value of 10.182 kWh is recorded in the forward direction.

A comparative analysis of the results (before and after adding PV) reveals an increase in energy consumption from 119.74kWh to 120.82kWh in forward and from 137.46kWh to 138.69kWh in return for an extra mass of 0.616 tone (around 1% of the total train mass). This difference in overall mass is around 0.89% in both directions. This led us to the conclusion that the integration of the PV panels slightly affects the energy required to move the total mass (tractive power) but provide a significant advantage as an alternative potential power supply which is environmentally friendly.

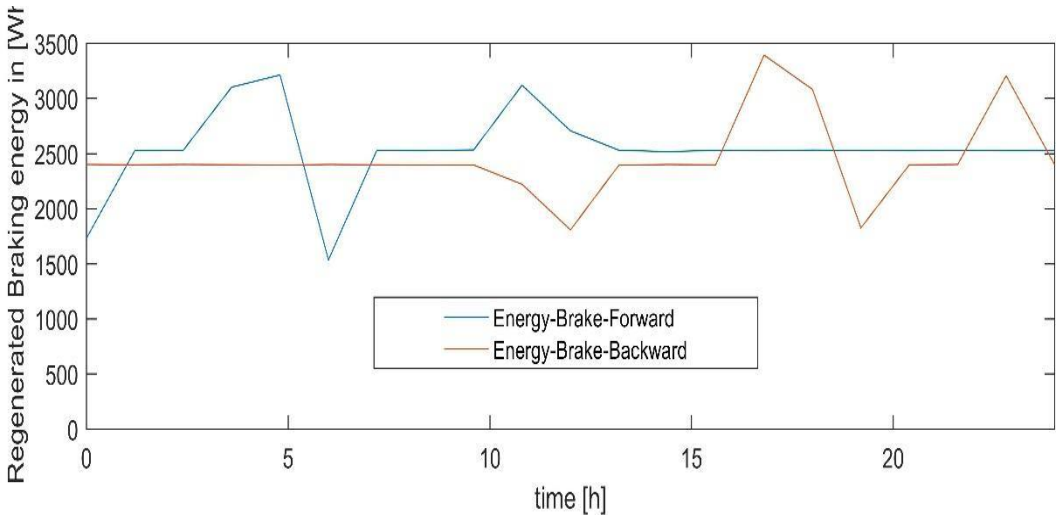

Figure 11. Regenerative Energy from braking

Figure 11 portrays the regenerative energy from braking, both forward and Return. We can realize from this figure that the area covered by the curves in both forward and Return directions are approximately the same. This may lead us to conclude that the energy regenerated from the braking system are almost equal. However, a slight difference materialized by a surplus production in average for the forward direction can be noticed. Note also that the energy from braking present less fluctuations and that helps to keep the system in a more stable and predictable mode.

For reliable system design, a worst-case scenario should always be taken into account. In our case, we have considered the highest energy demand which our system must satisfy. From the previous scenario, (before adding the PV panels), the highest energy demand was computed at the maximum speed. Therefore, the energy demand before adding the mass of the PV panels cannot be considered for accurate design.

So far, the energy consumption and regenerative have been computed by considering one-way trip for the train. The AALRT has in average fourteen trips per day (seven forward and seven return trips regularly). Table 3 show the average daily energy exchange considering the total number of daily trips for the E-W line.

Table 3 Average energy exchange

Average daily energy consumption [kWh] Total [kWh/day]	Forward	845.74
	Return	970.83
	Forward + Return	1, 816.57
Average daily regenerative energy [kWh/day] Total [kWh/day]	Forward	386.82
	Return	374.22
	Forward + Return	761.04

Energy exchange analysis	
Average daily energy production PV+Braking	53.76 + 761.04 = 814.8 kWh/day
Energy exchange	1 816.57 – 814.8 = 1,001.77 kWh/day

From table 3 we can see that from the total daily energy demand of 1,816.57kWh by a single vehicle, 814.8kWh namely 44.85% is produced by the PV systems together with regenerative braking. The network must be able to cater for the highest energy requirement at any time during the day. Therefore, the utility grid must come into play to supply the shortage of 1,001.77 kWh which is 55.15% of the total daily train energy demand. However, to allow this energy exchange, several parameters have to be considered for a good synchronization and power leakage avoidance which future studies should look at and the economic impact.

4. Conclusion

The paper studied the feasibility of supplying the Addis Ababa Light Rail Transit with solar panels. The goals of this study have been achieved through a set of systematic calculations and careful analysis. The total energy requirement for a single vehicle of the AALRT train has been computed on a daily basis and potential PV array on the roof of the vehicle has been carefully sized. The regenerative braking energy has also been calculated to contribute to the vehicle energy requirement as well. A demand-supply analysis has been carried out to assess the practicability of the proposed system. Finally, an energy exchange amongst the elements of the system has been accomplished to find out the necessity of installing supercapacitor batteries.

Results of the study have confirmed the possibility of incorporating the solar panels as an alternative supply. The demand-supply analysis has however shown that the total energy production comprising the PV energy and the regenerative braking energy always fall below the total energy demand by the train. This implies that the utility has to come into play to supply the shortage. It has also been concluded that the energy storage is not required for this particular case of study (AALRT). The energy storage could be needed for other train system that can accommodate a larger PV array.

Data Availability

All data, models and code generated or used during the study are available from the authors by request.

References

1. F. Ciccarelli, L. P. Di Noia, and R. Rizzo, "Integration of photovoltaic plants and supercapacitors in tramway power systems," Energies, vol. 11, no. 2, pp. 1–14, 2018, doi: 10.3390/en11020410.
2. G. K. G, "SOLAR TRAIN," Dep. Electron. Commun., vol. 6, no. 2, 2016.
3. M. Lencwe, S. D. Chowdhury, and H. M. Elgohary, "Solar Photovoltaic Integration on Locomotive Roof Top for South African Railway Industry," Conf. proceedings, IEEE, no. May 2019, 2016, doi: 10.1109/UPEC.2016.8114087.
4. M. Spiryagin, Q. Wu, P. Wolfs, Y. Sun, and C. Cole, "Comparison of locomotive energy storage systems for heavy-haul operation," Int. J. Rail Transp., vol. 00, no. 00, pp. 1–15, 2017, doi: 10.1080/23248378.2017.1325719.
5. N. B. Leo Murray, Powering our railways with Solar PV. 2017.
6. S. H. I. Jaffery, H. A. Khan, M. Khan, and S. Ali, "A study on the feasibility of solar powered railway system for light weight urban transport," World Renew. Energy Forum, WREF 2012, Incl. World Renew. Energy Congr. XII Color. Renew. Energy Soc. Annu. Conf., vol. 3, no. May, pp. 1892–1896, 2012.
7. N. Regis, "Optimal Battery Sizing of a Grid-Connected Residential Photovoltaic System for Cost Minimization using PSO Algorithm," Eng. Technol. Appl. Sci. Res., vol. 9, no. 6, pp. 4905–4911, 2019.
8. P. Gouthami, R. Dana, P. Elisa, B. B. Koo, K. Sandra, and F. Gina, "Beyond Connections: Energy Access Diagnostic Report Based on the Multi-Tier Framework," Int. Bank Reconstr. Dev. / World Bank, 2018, doi: 10.1596/24368.

9. E. M. Washing and S. S. Pulugurtha, "Energy demand and emission production comparison of electric , hydrogen and hydrogen- hybrid light rail trains," Int. J. Rail Transp., vol. 8378, no. February, 2016, doi: 10.1080/23248378.2015.1086554.
10. D. Gowda, S. S. Lokare, N. N. Kumbhar, B. Kolekar, and A. K. Teli, "MODIFICATIONS OF SOLAR TRAIN," Int. J. Sci. Res. Rev., vol. 7, no. 3, pp. 434–444, 2018.
11. M. Khodaparastan, S. Member, A. Mohamed, and S. Member, "Modeling and Simulation of Regenerative Braking Energy in DC Electric Rail Systems," 2018 IEEE Transp. Electrif. Conf. Expo, no. June, pp. 1–6, 2018, doi: 10.1109/ITEC.2018.8450133.
12. M. Khodaparastan, S. Member, A. A. Mohamed, S. Member, and W. Brandauer, "Recuperation of Regenerative Braking Energy in Electric Rail Transit Systems," IEEE Trans. Intell. Transp. Syst., vol. 7, pp. 1–16, 2018.
13. P. Vivek, N. B. Muthuselvan, and J. Nanadhagopal, "Modeling of Solar PV System for DC-DC Converter with improved voltage stability Using Hybrid - Optimization Techniques," in International Conference for Phoenixes on Emerging Current Trends in Engineering and Management (PECTEAM 2018) Modeling, 2018, no. January, doi: 10.2991/pecteam-18.2018.33.
14. S. Tesema, "Resource Assessment and Optimization Study of Efficient Type Hybrid Power System for Electrification of Rural District in Ethiopia," Int. J. Energy Power Eng., vol. 3, no. 6, p. 331, 2014, doi: 10.11648/j.ijepe.20140306.16.
15. E. Rohollahi, M. Abdolzadeh, and M. A. Mehrabian, "Prediction of the power generated by photovoltaic cells fixed on the roof of a moving passenger coach: A case study," Proc. Inst. Mech. Eng. Part F J. Rail Rapid Transit, vol. 229, no. 7, pp. 830–837, 2015, doi: 10.1177/0954409714524749.
16. B. L. Theraja, Chapter 43: Electric traction. 2003.
17. J. Wang and H. Rakha, "Electric Train Energy Consumption Modeling," Appl. Energy, no. May, 2017, doi: 10.1016/j.apenergy.2017.02.058.